

A Physical Model of the Turbulent Boundary Layer Consonant with the Structure of the Mean Momentum Balance

J. Klewicki,¹ P. McMurtry,¹ P. Fife² and T. Wei¹

¹Department of Mechanical Engineering, ²Department of Mathematics
University of Utah, Salt Lake City, Utah 84112 USA

Abstract

Recent studies by the present authors have explored, both empirically and analytically, the nature by which the terms in the mean momentum equation, as applied to canonical turbulent wall flows, sum to zero as a function of distance from the wall. To establish a context for the present work, the previously unrecognized structural and Reynolds number scaling properties revealed in these previous studies are succinctly reviewed. These characteristics are then used as the basis for composing a physical model for the turbulent boundary layer. The model is constructed such that it appropriately embraces the dynamical structure of the mean flow, while remaining consistent with independent empirical observations. Implications of the proposed model relative to the well-established view of boundary layer structure are briefly discussed.

Introduction

An established tack for describing turbulent wall flow structure begins with an examination of the distribution of the mean axial velocity as a function of distance from the wall, $U^+(y^+)$, in concert with an examination of the mean viscous stress profile, $\partial U^+/\partial y^+(y^+)$, relative to the magnitude of the Reynolds shear stress profile, $T^+(y^+) = -\overline{uv}^+(y^+)$. (In these expressions the superscript + denotes normalization by the kinematic viscosity, ν , and the friction velocity, $u_\tau = \sqrt{\tau_{wall}/\rho}$, with τ_{wall} and ρ being the mean wall shear stress and mass density respectively.) Such an analysis naturally leads to the well-accepted interpretations regarding the average dynamical characteristics of the constituent layers nearly universally employed to describe to boundary layer structure, e.g., [1]. Empirical data directly relevant to the mean momentum balance, however, reveal a layer structure that differs considerably from the sub, buffer, logarithmic and wake layers ascribed to the mean velocity profile [2]. Given this, the objectives of the present effort are to: *i*) outline the origin and basic features of this newly revealed dynamical layer structure, *ii*) propose a consistent physical model, and *iii*) briefly discuss the implications of this model relative to the more traditional view of boundary layer structure.

Review of Momentum Balance Properties

An important premise underlying the layer structure to be described, and, in turn, the proposed model, is that the Reynolds Averaged Navier-Stokes (RANS) equation in its unintegrated form (and in this case as applied to boundary layer flow over a planar surface located at $y = 0$),

$$U^+ \frac{\partial U^+}{\partial x^+} + V^+ \frac{\partial U^+}{\partial y^+} = \frac{\partial^2 U^+}{\partial y^{+2}} + \frac{\partial T^+}{\partial y^+}, \quad (1)$$

provides the primary description of mean flow dynamics. (Herein, x is the axial coordinate, y is the wall normal coordinate, U and V are the velocity components in the x and y directions respectively, upper case letters represent mean quantities, lower case letters denote fluctuating quantities, tilde denotes instantaneous quantities (i.e.,

$\bar{u} = U + u$), an overbar denotes time averaging, and vorticity components are identified by their subscript.) The left side of Eq. 1 represents mean flow advection, while the right side terms represent the viscous and Reynolds stress gradients respectively. Since, for the flat plate flow, there are only these three distinct dynamical effects, the ratio of any two determine the nature by which the equation is balanced.

Layer Structure

Wei et al. [2] explored the structure of boundary layer, pipe and channel flows by examining the ratio of the last two terms in Eq. 1. Interpretation of this ratio is as follows:

1. If $|\frac{\partial^2 U^+}{\partial y^{+2}} / \frac{\partial T^+}{\partial y^+}| \gg 1$ then the Reynolds stress gradient term is negligible and Eq. 1 sums to zero essentially through a balance of the mean advection and viscous stress gradient terms.
2. If $|\frac{\partial^2 U^+}{\partial y^{+2}} / \frac{\partial T^+}{\partial y^+}| \ll 1$ then the mean viscous stress gradient term is negligible and Eq. 1 sums to zero essentially through a balance of the mean advection and Reynolds stress gradient terms.
3. If $|\frac{\partial^2 U^+}{\partial y^{+2}} / \frac{\partial T^+}{\partial y^+}| \simeq 1$ then the Reynolds stress and viscous stress gradients balance and are either greater or of the same order of magnitude as the mean advection term.

Relevant premier quality experimental and DNS data [3, 4, 5] were differentiated and the indicated ratio was examined as a function of distance from the wall, $y^+ = yu_\tau/\nu$, for differing Reynolds numbers, δ^+ , where δ is the boundary layer thickness.

The sketch of Figure 1 depicts the behavior of the stress gradient ratio at any fixed δ^+ . As indicated, there exists a four layer structure. Layer I retains the character of the viscous sublayer, and in the boundary layer is a region where the viscous stress gradient nominally balances mean advection. In layer II the magnitude of the ratio is very close to unity, and thus is called the stress gradient balance layer. Across the mesolayer (layer III), the Reynolds stress gradient changes sign and the terms in Eq. 1 undergo a process of balance breaking and exchange [2, 6]. The net result of this process is that from the outer edge of layer III to $y = \delta$ (i.e., layer IV) Eq. 1 is characterized by a balance between mean advection and turbulent transport via the Reynolds stress gradient.

Reynolds Number Scaling Behaviors

The qualitative features of Fig. 1, depicted for a fixed Reynolds number, persist for the Reynolds number range currently accessible to inquiry. Quantitatively, however, this layer structure has been shown [2] to exhibit distinct Reynolds number dependencies relating to both the wall-normal extent of the layers and the velocity increment across each of the layers. Table 1 presents these scaling behaviors as normalized by inner variables. As is evident, layers I

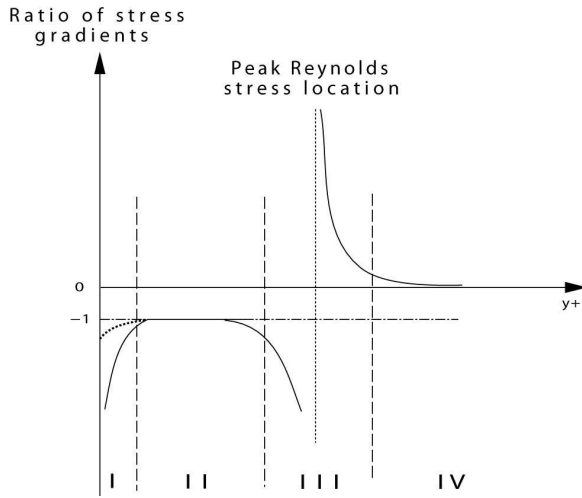


Figure 1: Sketch of the ratio of the viscous stress gradient to the Reynolds stress gradient (terms on the right side of Eq. 1) in a turbulent boundary layer at any given Reynolds number. Layer I is characterized by a balance between mean advection and the viscous stress gradient; dashed line. (Note that in a pipe this balance is between the mean pressure gradient and the viscous stress gradient.) In layer II the balance is between the viscous and Reynolds stress gradients. Layer III is a mesolayer in which all three terms in Eq. 1 are of the same order of magnitude, except that in a part of it, the Reynolds stress gradient is negligible. Layer IV is defined by a balance between mean advection and turbulent inertia.

and IV adhere (at least asymptotically) to the traditional inner and outer scalings respectively. On the other hand, layers II and III exhibit mixed scaling properties. The inner normalized thickness of layer II grows like the geometric mean of the Reynolds number defined as the ratio of outer to inner length scales (i.e., $\sim \sqrt{\delta^+}$), while its velocity increment remains a fixed fraction of U_∞ , independent of Reynolds number. Similarly, $\Delta_{III}y^+ \sim \sqrt{\delta^+}$, while its velocity increment is only about $1.0u_\tau$, independent of δ^+ . As discussed in detail by Wei et al. [2], these scaling behaviors differ considerably from the classical view of boundary layer structure, and are associated with the existence of a third fundamental length scale, $\sqrt{\nu\delta^+/u_\tau}$, that is intermediate to ν/u_τ and δ .

layer	Δy^+ increment	ΔU^+ increment
I	$\mathcal{O}(1)$ ($\simeq 3$)	$\mathcal{O}(1)$ ($\simeq 3$)
II	$\mathcal{O}(\sqrt{\delta^+})$ ($\simeq 1.6\sqrt{\delta^+}$)	$\mathcal{O}(U_\infty^+)$ ($\simeq U_\infty^+/2$)
III	$\mathcal{O}(\sqrt{\delta^+})$ ($\simeq 1.0\sqrt{\delta^+}$)	$\mathcal{O}(1)$ ($\simeq 1$)
IV	$\mathcal{O}(\delta^+)$ ($\rightarrow \delta^+$)	$\mathcal{O}(U_\infty^+)$ ($\rightarrow U_\infty^+/2$)

Table 1: Inner-normalized scaling behaviors of the layer thicknesses and velocity increments. Note that the layer IV properties are asymptotically attained as $\delta^+ \rightarrow \infty$.

The mean dynamics and scaling behaviors associated with layers II and III are central and apparently unique to the model proposed below, and thus are worthy of further discussion. Layer II is called the stress gradient balance layer since the dominant dynamical mechanisms are the viscous and Reynolds stress gradient terms on the right of Eq. 1; underlying their ratio being -1 in Fig. 1. Contrary to the prevalent notion that boundary layer dynamics are inertially dominated outside the buffer layer (independent of δ^+), momentum balance data incontrovertibly reveal that an equal competition between viscous and inertial effects persists to a wall-normal distance near the peak in the Reynolds stress, T_{max} . Consistent with

the mathematical hierarchical structure revealed by Fife et al. [6], in the model posed below this competition is associated (in a time mean sense) with the vortical motions forming and evolving from the near-wall vorticity field. It is significant to note, however, that the balance in layer II comes about via two nearly equal but opposite decreasing functions that lose their dominance over mean advection as layer II transitions into layer III.

The scalings of Table 1 reveal that the layer II and III thicknesses are coupled such that their velocity increments adhere to outer and inner scaling respectively. These properties underlie new interpretations relating to, for example, the nature of the inner/outer interaction in boundary layers. In this regard it is relevant to note that major portions of layers II and IV and all of layer III reside within the bounds of the region of the mean profile that exhibits a logarithmic-like variation with y^+ . The lower edge of layer II is fixed near the edge of the viscous sublayer (independent of δ^+), while the position of its outer edge extends to increasing y^+ values like $\sqrt{\delta^+}$ such that $\Delta_{II}U = U_\infty/2$. (Note that relative to outer scaling the position of the outer edge of layer II moves “inward” like $1/\sqrt{\delta^+}$.) Because of this positioning behavior for layer II, both end points of layer III vary with δ^+ . Thus, while the layer III thickness exhibits the same Reynolds number scaling behavior as layer II, its velocity increment is only $\simeq 1u_\tau$ owing to the fact that with increasing δ^+ its position is located at increasing y^+ locations in a region where $U^+ \simeq \log(y^+)$.

Physical Model

Elements of a new physical model for the boundary layer are presented in the schematic of Figure 2. In contrast to the physical picture promoted by the traditional (sub, buffer, log and wake layer) view, this model is consistent with the properties of the mean momentum balance reviewed above. Associated with this are requisite nontrivial reinterpretations and modified insights relating to the description of flow physics. Conversely, it is recognized that any defensible model should also embrace the numerous independent empirical observations relating to, for example, boundary layer coherent motions. As evidenced below, the model presented in Figure 2 attempts to simultaneously satisfy these constraints.

A particularly prevalent and growing body of research supports the hypothesis that hairpin-like vortices constitute a basic building block of wall turbulence, e.g., [7, 8, 9, 10, 11, 12]. Broadly speaking, near-wall hairpin vortices are seen to form via redistribution of the intense sublayer vorticity field (mainly composed of $\tilde{\omega}_z$), and during their development extend outward. While earlier flow visualization-based evidence indicated that these motions might extend from the sublayer to the edge of the boundary layer [9], an increasing and predominantly more recent body of results indicates that at some distance from the wall the boundary layer vortical motions lose connection with their sublayer/near-wall origin.

This “attached” – “detached” eddy decomposition of the vorticity field finds support from visual studies [13, 14, 15, 16], two-point vorticity correlations [14, 17, 18] and DNS and PIV studies [19, 12, 20]. Furthermore, the inclusion of detached eddies has been found to improve coherent motion-based model performance [21]. As depicted in Fig. 2, attached eddies are viewed as predominantly populating layer II, and to a decreasing degree with increasing y^+ across layer III and into layer IV. Though a specific geometric form for the detached eddies is not completely established, direct measurements of near-wall $\tilde{\omega}_z$ structure, the increasingly three-dimensional nature of the vorticity field with increasing distance from the surface, and data considerations relative to $\vec{\nabla} \cdot \vec{\omega} = 0$ [22, 23, 16] support the expectation that at some distance from wall the characteristic coherent vortical motions become spatially localized and topologically form closed loops. Detached ed-

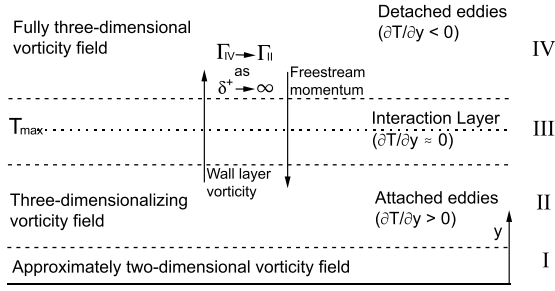


Figure 2: Schematic representation of some of the dynamical attributes of the proposed model for the turbulent boundary layer. Layer numbers are the same as those identified in Fig. 1.

dies are hypothesized to predominantly populate layer IV, and to a decreasing degree with decreasing y^+ across layer III and into layer II. Of course, the simplest form of such an eddy is a vortex ring-like motion. Falco’s earlier “typical eddy” observations [13, 15] support the existence of intermediate scale ring-like eddies in both the inner and outer regions. More recently, direct numerical simulations by Bake et al. [24] provide compelling evidence for the formation of vortex rings from the pinch-off of the legs of hairpin vortices during the latest stages of transition. Such a process was previously proposed by Falco as a mechanism for ring-like motion formation, and was explored numerically by Moin et al. [25]. Regardless of the exact geometric form of the detached eddies, however, an important characteristic feature is hypothesized to be that they contain positive $\tilde{\omega}_z$, i.e., having sign opposite Ω_z [14, 22, 26, 17, 18].

The new insights derived from the properties of the mean momentum balance [2, 6] allow specific attributes to be associated with the attached/detached eddy structure proposed. For example, under the proposed model attached eddies form and evolve across layer II, and thus their dynamical signature is that they produce instantaneous contributions to positive $-\partial\overline{uv}/\partial y$. Similarly, the characteristic eddies of layer IV are detached. Therefore their dynamical signature is that they produce negative $-\partial\overline{uv}/\partial y$.

In the context of these dynamical signatures it is useful to examine the equation, e.g., [27, 28],

$$-\frac{\partial\overline{uv}}{\partial y} = \overline{v\omega_z} - \overline{w\omega_y} + \frac{\partial}{\partial x}(\overline{v^2} + \overline{w^2} - \overline{u^2}). \quad (2)$$

For turbulent channel flow the last term is identically zero, while for boundary layers this term is small, especially as δ^+ becomes large [28]. Thus, to a very good approximation, the gradient of the Reynolds stress is established by the difference of the indicated velocity vorticity correlations. Given this, the interpretation is that in layer II the attached eddies interact with the velocity field to generate a net positive sum, and in layer IV the detached eddies generate a net negative sum. The dominant terms in Eq. 1 indicate that the dynamics underlying the evolution of attached eddies are characterized by a competition between viscous shear forces and turbulent advection. Similarly, detached eddy dynamics in layer IV are characterized by a competition between mean flow and turbulent advection. The flow field interactions underlying Eq. 2 in either layer II or layer IV have recently been shown to be intermediate in scale [29]. Physically, the reason for this is attributable the fact that as $\delta^+ \rightarrow \infty$ velocity spectra peak at decreasingly low wavenumber, while vorticity spectra peak at increasingly high wavenumber. According to Eq. 2, however, the velocity and vorticity fields must interact (i.e., correlate) over some wavenumber range in order for there to be a

net momentum transport via turbulent inertia.

Discussion

The proposed model creates a new context for describing boundary layer processes. In this regard, three important issues are now briefly discussed. These concern *i*) inner/outer interactions, *ii*) coherent motion dynamics, and *iii*) scaling turbulence statistics. A more comprehensive discussion these issues in the context of the proposed model is forth-coming [30].

Given the proposed physical model, a central element of the inner/outer interaction would seem to have association with how the attached and detached eddies interact, and, in particular, how these interactions simultaneously accomplish a net outward transport of vorticity (associated with boundary layer growth) and a net inward transport of momentum (associated with the surface drag). The proposed model provides a rather clearly defined framework for identifying where in the layer the inner/outer interaction occurs (as a function of Reynolds number) and the competing mean dynamical effects at play. Overall, the velocity increment scalings suggest that as $\delta^+ \rightarrow \infty$ a net outcome of the interaction is that the circulation (per unit length) associated with the outward transport of vorticity from layer II is asymptotically balanced by the net inward transport of momentum from layer IV.

Relevant to coherent motion dynamics, important questions would appear to relate to how the instantaneous dynamics of attached eddies produce the statistical features of layer II, and similarly how detached eddies produce the negative Reynolds stress gradient of layer IV. The respective physical interpretations (in the context of Eq. 2) are that *i*) the vortical motions in the region inside of T_{max} interact with the velocity field to act as a source term in Eq. 1, and *ii*) the vortical motions for y^+ values greater than the position of T_{max} interact with the velocity field to act as a sink term.

Connected to the above *instantaneous-to-mean* perspectives is the somewhat converse issue of scaling turbulence quantities using the properties of the mean flow. That is, given the Reynolds number dependencies of the mean momentum field described above, such connections would permit the prediction of turbulence properties at arbitrary δ^+ . Relative to this, it is worth noting that the scaling hierarchy revealed by the analysis of Fife et al. [6] provides new insights. Furthermore, the layer scaling behaviors reflected in Table 1 constitute a broader set of velocity and length scale combinations than contained in the traditionally employed theory based on the assumption of a region of inner and outer overlap.

Conclusions

A new framework for interpreting boundary layer dynamics is described herein. Notable features of this model include and incorporate the following.

- The y^+ extent of the dynamical interaction characterized by a balance between viscous/inertial effects (Layer II) is both Reynolds number dependent and, in general, much larger than previously recognized in the traditional layer structure ascribed to boundary layers.
- Both the y^+ position and extent of the region over which the inner/outer interaction occurs is Reynolds number dependent. The inner/outer interaction primarily occurs over a region in which the terms in the mean momentum equation undergo the balance breaking and exchange as described by Fife et al. [6].
- The Reynolds stress gradient has opposite dynamical contributions to the mean momentum equation for y^+ positions on

the inside and outside of T_{max} respectively.

- To be fully understood, the dynamical layer structure of the mean momentum balance requires an extended/revised set of length and velocity information. These provide a broader context for scaling turbulence quantities.

Acknowledgements

This work was supported by the National Science Foundation under grant CTS-0120061 (grant monitor, M. Plesniak), the Office of Naval Research under grant N00014-00-1-0753 (grant monitor, R. Joslin), and the Department of Energy under grant W-7405-ENG-48.

References

- [1] Pope, S.B., *Turbulent Flow*, Cambridge University Press, 2000.
- [2] Wei, T., Fife, P., Klewicki, J. and McMurtry, P., Properties of the mean momentum balance in turbulent boundary layer, pipe and channel flows, *J. Fluid Mech.*, to appear, 2004.
- [3] Moser, R.D., Kim, J. and Mansour, N.N., Direct numerical simulation of turbulent channel flow up to $R_\tau = 590$, *Phys. Fluids*, **11**, 1999, 943.
- [4] Zagarola, M.V. and Smits, A.J., Scaling of the mean velocity profile for turbulent pipe flow, *Phys. Rev. Lett.*, **78**, 1997, 239.
- [5] DeGraaff, D.B. and Eaton, J.K., Reynolds number scaling of the flat plate turbulent boundary layer, *J. Fluid Mech.*, **422**, 2000, 319.
- [6] Fife, P., Wei, T., Klewicki, J. and McMurtry, P., Stress gradient balance layers and scale hierarchies in wall bounded turbulent flows, *J. Fluid Mech.*, submitted, 2004.
- [7] Theodorsen, T., Mechanism of turbulence, in *2nd Midwestern Conference on Fluid Mechanics*, The Ohio State University, Columbus, OH, 1952, 1.
- [8] Wallace, J.M., On the structure of turbulent shear flow. A personal view, in *Developments in Theoretical and Applied Mechanics*, editors Chung, T.J. and Karr, G., University of Alabama, Department of Mechanical Engineering, Huntsville, Alabama, 1982, 1.
- [9] Head, M.R. and Bandyopadhyay, P., New aspects of turbulent boundary layer structure, *J. Fluid Mech.*, **107**, 1981, 297.
- [10] Perry, A.E., Henbest, S. and Chong, M.S., A theoretical and experimental study of wall turbulence, *J. Fluid Mech.*, **165**, 1986, 163.
- [11] Smith, C.R., Walker, J.D.A., Haidari, A.H. and Sobrun, U., On the dynamics of near-wall turbulence, *Phil. Trans. R. Soc. Lond. A*, **336**, 1991, 131.
- [12] Adrian, R.J., Meinhart, C.D. and Tomkins, C.D., Vortex organization in the outer region of the turbulent boundary layer, *J. Fluid Mech.*, **422**, 2000, 1.
- [13] Falco, R.E., New results, a review and synthesis of the mechanism of turbulence production in boundary layers and its modification, *AIAA paper no. 83-0377*, 1983.
- [14] Klewicki, J.C., *On the Interactions Between the Inner and Outer Region Motions in Turbulent Boundary Layers*, Ph.D. Dissertation, Michigan State University, 1989.
- [15] Falco, R.E., A coherent structure model of the turbulent boundary layer and its ability to predict Reynolds number dependence, *Phil. Trans. R. Soc. Lond. A*, **336**, 1991, 103.
- [16] Klewicki, J.C., Self-sustaining traits of near-wall motions underlying boundary layer stress transport, in *Self-sustaining mechanisms of wall turbulence*, editor Panton, R.L., Computational Mechanics Publications, Southampton, UK, 1997, 135.
- [17] Klewicki, J.C. and Falco, R.E., Spanwise vorticity structure in turbulent boundary layers, *Int. J. Heat and Fluid Flow*, **17**, 1996, 363.
- [18] Metzger, M.M. and Klewicki, J.C., A comparative study of wall region structure in high and low Reynolds number turbulent boundary layers, *Phys. Fluids*, **13**, 2001, 692.
- [19] Robinson, S.K., Coherent motions in the turbulent boundary layer, *Ann. Rev. Fluid Mech.*, **23**, 1990, 601.
- [20] Ganapathisubramani, B., Longmire, E.K. and Marusic, I., Characteristics of vortex packets in turbulent boundary layers, *J. Fluid Mech.*, **478**, 2003, 35.
- [21] Perry, A.E. and Marusic, I., A wall-wake model for the turbulence structure of boundary layers. Part 1. Extension of the attached eddy hypothesis, *J. Fluid Mech.*, **298**, 1995, 361.
- [22] Klewicki, J.C., Gendrich, C.P., Foss, J.F. and Falco, R.E., On the sign of the instantaneous spanwise vorticity component in the near-wall region of turbulent boundary layers, *Phys. Fluids A*, **2**, 1990, 1497.
- [23] Rajagopalan S. and Antonia, R.A., Structure of the velocity field associated with the spanwise vorticity in the wall region of a turbulent boundary layer, *Phys. Fluids A*, **5**, 1993, 2502.
- [24] Bake, S., Meyer, D.G.W. and Rist, U., Turbulence mechanism in Klebanoff transition: a quantitative comparison of experiment and direct numerical simulation, *J. Fluid Mech.*, **459**, 2002, 217.
- [25] Moin, P., Leonard, A. and Kim, J., Evolution of a curved vortex filament into a vortex ring, *Phys. Fluids*, **29**, 1986, 955.
- [26] Klewicki, J.C., Murray, J.M. and Falco, R.E., Vortical motion contributions to stress transport in turbulent boundary layers, *Phys. Fluids*, **6**, 1994, 277.
- [27] Hinze, J.O., *Turbulence*, McGraw-Hill, 1975.
- [28] Klewicki, J.C., Velocity-vorticity correlations related to the gradients of the Reynolds stress in parallel turbulent wall flows, *Phys. Fluids A*, **1**, 1989, 1285.
- [29] Priyadarshana, P. and Klewicki, J.C., Reynolds number scaling of wall layer velocity-vorticity products, in *Reynolds Number Scaling in Turbulent Flow*, editor Smits, A.J., Kluwer Academic Publishers, 2003, 117.
- [30] Klewicki, J., McMurtry, P., Fife, P. and Wei, T., Physical models of wall turbulence consonant with the dynamical structure of the mean flow, *J. Fluid Mech.*, in preparation.